

for 1 h. As soon as  $K_2CO_3$  was added,  $CO_2$  started to evolve. Addition of THF into the resulting colorless solution produced a white solid (yield 92%). Elemental analysis calcd (%) for  $CH_3KSe$ : C 6.6, H 1.7, K 21.5, Se 43.6; found: C 6.8, H 1.8, K 21.4, Se 42.7;  $^1H$  NMR (300 MHz,  $[D_4]methanol$ , 25 °C):  $\delta$  = 3.35 (s).

Single crystals of **1** suitable for X-ray diffraction studies were grown inside a dry-box (under argon). Compound **1** (0.5 g) was dissolved in methanol (3 mL) in a vial which was contained within a larger vial charged with approximately 2 mL of diethyl ether. The diethyl ether was allowed to slowly diffuse into the methanol solution by maintaining the vials at room temperature for several days.

**2a**: A solution of (bmim)Cl (3.1 g, 18 mmol) in methanol (30 mL) was treated with 1.1 equiv of **1** (3.6 g, 19.8 mmol) in methanol (30 mL) at room temperature. After stirring for 6 h, the solution was filtered to remove KCl and the solvent was evaporated under reduced pressure to give a yellow liquid. The resulting liquid was further purified by adding  $CH_2Cl_2$  and filtering to remove excess **1** and KCl, followed by drying under high vacuum for 12 h (yield 85%). Elemental analysis calcd (%) for  $C_9H_{18}N_2Se$ : C 38.45, H 6.41, N 9.97, Se 28.09; found: C 38.18, H 6.30, N 9.60, Se 28.10;  $^1H$  NMR (300 MHz,  $CDCl_3$ , 25 °C):  $\delta$  = 0.91 (t,  $^3J(H,H)$  = 7.5 Hz, 3H;  $CH_3$ ), 1.34 (m, 2H;  $CH_2$ ), 1.83 (m, 2H;  $CH_2$ ), 3.45 (s, 3H;  $OCH_3$ ), 4.06 (s, 3H;  $NCH_3$ ), 4.27 (t,  $^3J(H,H)$  = 7.2 Hz, 2H;  $NCH_2$ ), 7.23 (d,  $^3J(H,H)$  = 1.5 Hz, 1H;  $C_3H_3N_2$ ), 7.33 (d,  $^3J(H,H)$  = 1.5 Hz, 1H;  $C_3H_3N_2$ ), 10.58 ppm (s, 1H;  $C_3H_3N_2$ ); LC-MS ( $CH_3OH$ ): positive ion: 139 [bmim] $^+$ ; negative ion: 143 [ $SeO_2(OCH_3)$ ] $^-$ .

**3a** and **4a** were prepared in a similar manner to that of **2a**, by replacing (bmim)Cl with (emim)Cl and (dmim)Cl, respectively.

**3a**: Yield 86%; elemental analysis calcd (%) for  $C_7H_{14}N_2Se$ : C 33.21, H 5.54, N 11.07, Se 31.20; found: C 32.90, H 5.50, N 11.50, Se 29.70;  $^1H$  NMR (300 MHz,  $CDCl_3$ , 25 °C):  $\delta$  = 1.51 (t,  $^3J(H,H)$  = 7.8 Hz, 3H;  $CH_3$ ), 3.47 (s, 3H;  $OCH_3$ ), 4.04 (s, 3H;  $NCH_3$ ), 4.35 (q,  $^3J(H,H)$  = 7.5 Hz, 2H;  $NCH_2$ ), 7.28 (s, 1H;  $C_3H_3N_2$ ), 7.30 (s, 1H;  $C_3H_3N_2$ ), 10.88 ppm (s, 1H;  $C_3H_3N_2$ ). LC-MS ( $CH_3OH$ ): Positive ion: 111 [emim] $^+$ ; Negative ion: 143 [ $SeO_2(OCH_3)$ ] $^-$ .

**4a**: Yield 87%; elemental analysis calcd (%) for  $C_6H_{12}N_2Se$ : C 30.14, H 5.02, N 11.72, Se 33.03; found: C 30.00, H 5.00, N 11.90, Se 32.10;  $^1H$  NMR (300 MHz,  $CDCl_3$ , 25 °C):  $\delta$  = 3.45 (s, 3H;  $OCH_3$ ), 3.98 (s, 6H; 2( $NCH_3$ )), 7.31 (s, 2H;  $C_3H_3N_2$ ), 10.83 ppm (s, 1H;  $C_3H_3N_2$ ). LC-MS ( $CH_3OH$ ): Positive ion: 97 [dmim] $^+$ ; Negative ion: 143 [ $SeO_2(OCH_3)$ ] $^-$ .

Transformation reactions of **3a** to give **3b** and **3c**:<sup>[10]</sup> A solution of **3a** (0.1 g, 0.4 mmol) in  $CH_3CH_2OH$  (3 mL) or  $CF_3CH_2OH$  (3 mL) was stirred at room temperature for 6 h, followed by removal of the solvent under high vacuum for 12 h to give a yellow liquid (yield 99%).

Transformation of **3a** to give **3d**:<sup>[10]</sup> A solution of **3a** (0.1 g, 0.4 mmol) in  $CH_2Cl_2$  (3 mL) was treated with 1.3 equiv of PhOH (0.05 g, 0.52 mmol) at room temperature for 6 h. The subsequent removal of the solvent and excess PhOH under high vacuum for 12 h gave a yellow liquid (yield 99%).

Catalysis reaction: All of the carbonylation reactions were conducted in a 100-mL Parr reactor with a magnetic drive stirrer and an electrical heater. The reactor was charged with an aromatic amine, methanol, an appropriate catalyst and toluene (1 mL) as an internal standard. The reactor was pressurized with a gaseous mixture of  $O_2$  and CO (20:80 v/v), and then heated to a specified temperature. The pressure was maintained at 1.4 MPa throughout the reaction using a reservoir tank equipped with a high-pressure regulator and a pressure transducer. After the reaction was completed, the reactor was cooled to room temperature and the reaction mixture was filtered off to remove the solid diaryl urea. The resulting solution and the isolated urea were analyzed by GC, HPLC, and GC-MS. Recycling experiment: The 100-mL reactor was charged with aniline (40 mmol), methanol (25 mL), **3a**, and toluene (1 mL) as the internal standard, and then reacted at 60 °C for 2 h under pressure of 1.4 MPa of  $O_2$ /CO (20:80 v/v). When the reaction was completed, diphenylurea was removed by filtration and the solution that contained the ionic liquid was reused for further carbonylation reactions with a fresh charge of consumed aniline.

Received: June 20, 2002

Revised: August 1, 2002 [Z19573]

- [1] a) A. M. Tafesh, J. Weiguny, *Chem. Rev.* **1996**, *96*, 2035–2052; b) J. D. Gargulak, W. L. Gladfelter, *Organometallics* **1994**, *13*, 698–705; c) I.

Vauthey, F. Valot, C. Gozzi, F. Fache, M. Lemaire, *Tetrahedron Lett.* **2000**, *41*, 6347–6350.

- [2] a) T. W. Leung, B. D. Dombek, *J. Chem. Soc. Chem. Commun.* **1992**, 205–206; b) K. V. Prasad, R. V. Chaudhari, *J. Catal.* **1994**, *145*, 204–215.  
[3] a) H. S. Kim, Y. J. Kim, H. Lee, K. Y. Park, C. S. Chin, *J. Catal.* **1998**, *176*, 264–266; b) H. S. Kim, Y. J. Kim, H. Lee, S. D. Lee, C. S. Chin, *J. Catal.* **1999**, *184*, 526–534.  
[4] a) R. Sheldon, *Chem. Commun.* **2001**, 2399–2407; b) C. M. Gordon, *Appl. Catal. A* **2001**, *222*, 101–117; c) R. J. C. Brown, P. J. Dyson, D. J. Ellis, T. Welton, *Chem. Commun.* **2001**, 1862–1863; d) J. E. L. Dullius, P. A. Z. Suarez, S. Einloft, R. F. de Souza, J. Dupont, *Organometallics* **1998**, *17*, 815–819; e) C. J. Adams, M. J. Earle, K. R. Seddon, *Chem. Commun.* **1999**, 1043–1044.  
[5] X-ray single-crystal diffraction data for **1** was collected on a Siemens SMART CCD diffractometer. Crystal data for **1**: monoclinic, space group  $P2_1/c$ ,  $a$  = 10.2502(16),  $b$  = 7.3115(12),  $c$  = 6.4330(10) Å,  $\beta$  = 103.012(2)°,  $V$  = 469.74(13) Å<sup>3</sup>,  $Z$  = 2,  $\rho_{\text{calcd}}$  = 2.561 g cm<sup>-3</sup>,  $\mu(Mo_{K\alpha})$  = 8.746 mm<sup>-1</sup>,  $R1$  = 0.0332,  $wR2$  = 0.0886, ( $I > 2\sigma(I)$ );  $R1$  = 0.0340,  $wR2$  = 0.0893 (all data). CCDC-185119 contains the supplementary crystallographic data for this paper. These data can be obtained free of charge via [www.ccdc.cam.ac.uk/conts/retrieving.html](http://www.ccdc.cam.ac.uk/conts/retrieving.html) (or from the Cambridge Crystallographic Data Centre, 12, Union Road, Cambridge CB2 1EZ, UK; fax: (+44) 1223-336-033; or deposit@ccdc.cam.ac.uk).  
[6] R. Hagiwara, Y. Ito, *J. Fluorine Chem.* **2000**, *105*, 221–227.  
[7] S. Fukuoka, M. Chono, M. Kohno, *J. Chem. Soc. Chem. Commun.* **1984**, 399–400.  
[8] a) S. A. Akyüz, A. B. Dempster, R. L. Morehouse, N. Zengin, *J. Chem. Soc. Chem. Commun.* **1972**, 307–308; b) N. Sonoda, T. Yasuhara, K. Kondo, T. Ikeda, S. Tsutsumi, *J. Am. Chem. Soc.* **1971**, *93*, 6344; c) K. Kondo, N. Sonoda, K. Yoshida, M. Koishi, S. Tsutsumi, *Chem. Lett.* **1972**, 401–404; d) J. G. Zajacek, J. J. McCoy, K. E. Fuger, *USP* 3956360 **1976**.  
[9] a) M. Hasan, I. V. Kozhevnikov, M. R. H. Siddiqui, A. Steiner, N. Winterton, *Inorg. Chem.* **1999**, *38*, 5637–5641; b) J. S. Wilkes, J. A. Levinsky, R. A. Wilson, C. L. Hussey, *Inorg. Chem.* **1982**, *21*, 1263–1264.  
[10] See the Supporting Information for the  $^1H$  NMR data of the transformation reactions of **3a** into **3b**, **3c**, and **3d**.

## Spatially Directed Protein Adsorption by Using a Novel, Nanoscale Surface Template\*\*

Patricia Moraille and Antonella Badia\*

Phase-separated, ultrathin organic films can serve as surface templates for the selective and patterned deposition of macromolecules on the submicron scale.<sup>[1–6]</sup> Deposition is generally directed by chemical differences in the domains or domain edges generated by phase separation. We demonstrate herein that a chemically *homogeneous* surface exhibiting solid/fluid-phase coexistence can also be used as an

[\*] Prof. A. Badia, P. Moraille  
Department of Chemistry, Université de Montréal  
C.P. 6128, succursale Centre-ville, Montréal, QC H3C 3J7 (Canada)  
Fax: (+1) 514-343-7586  
E-mail: antonella.badia@umontreal.ca

[\*\*] This work was supported by the NSERC (Canada), the FCAR (Québec), the CFI (Canada), and the Université de Montréal. A.B. is a Cottrell Scholar of the Research Corporation. P.M. gratefully acknowledges salary support from VRQ-NanoQuébec.



Supporting information for this article is available on the WWW under <http://www.angewandte.org> or from the author.

adsorption template. This greatly expands the repertoire of template composition and pattern form usable.

The adsorption template used in this study consists of nanoscale, parallel stripes generated by the Langmuir–Blodgett (LB) transfer of a mixed phospholipid monolayer from the air–water (A/W) interface onto a solid substrate.<sup>[7]</sup> This regular stripe pattern is composed of two saturated dialkylphosphatidylcholines, *L*- $\alpha$ -dipalmitoylphosphatidylcholine (DPPC) and *L*- $\alpha$ -dilauroylphosphatidylcholine (DLPC), in different phases.

The adsorption of human serum albumin (HSA) and human  $\gamma$  globulin (HGG) to the DPPC/DLPC monolayers was investigated. These blood-plasma proteins bind to alkylated surfaces either through specific interactions with alkyl-chain binding pockets (HSA) or through hydrophobic interactions (HSA and HGG).<sup>[8–11]</sup> This study was motivated by the possibility of spatially directing protein adsorption through differences in the alkyl-chain packing density and/or surface energies of the condensed versus fluid phases of mixed phospholipid monolayers.<sup>[12,13]</sup> We report herein the generation of novel protein and Au nanoparticle/protein patterns based on the selective adsorption of HSA and HGG to the liquidlike phase of the stripe pattern.

Monolayers, formed by the compression of binary mixtures of DPPC and DLPC at the A/W interface, were deposited onto mica by the LB technique. Films were transferred at surface pressures of 15 mN m<sup>-1</sup> and 32 or 35 mN m<sup>-1</sup>, which correspond to the liquid-condensed (LC) and solid-condensed (SC) phase of DPPC, respectively.<sup>[14]</sup> DLPC is in a liquid-expanded (LE) or fluid state at these surface pressures.<sup>[15]</sup> In the resulting LB films, the phosphocholine headgroups are adsorbed onto the mica and the lipid alkyl chains extend vertically from the surface. The protein solution thus “sees” a surface of alkyl chains terminated with CH<sub>3</sub> groups.

Typical atomic force microscopy (AFM) images of 0.25/0.75 and 0.50/0.50 (mol mol<sup>-1</sup>) DPPC/DLPC monolayers transferred at 35 mN m<sup>-1</sup> and 15 mN m<sup>-1</sup>, respectively, are presented in Figure 1. Parallel stripes (continuous and broken) protrude from the background matrix by  $\sim 0.9$  nm. The stripes are  $160 \pm 60$  nm wide for 0.25/0.75 DPPC/DLPC and  $210 \pm$

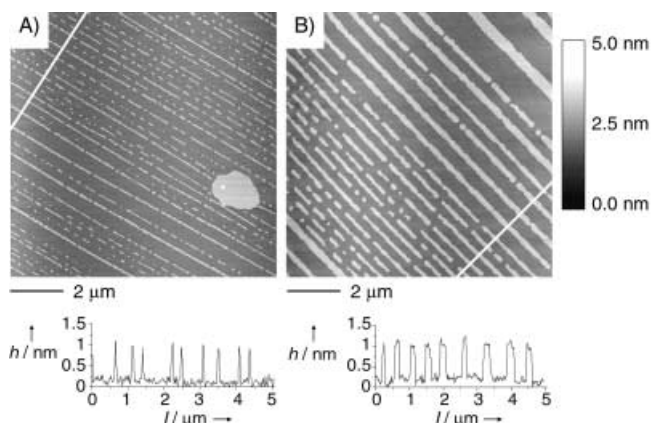


Figure 1. Top: AFM images of monolayers deposited on mica at 20°C: A) 0.25/0.75 (mol mol<sup>-1</sup>) DPPC/DLPC, 35 mN m<sup>-1</sup>; B) 0.50/0.50 (mol mol<sup>-1</sup>) DPPC/DLPC, 15 mN m<sup>-1</sup>; right: height scale. Bottom: Height-length profiles (step-heights: A)  $0.89 \pm 0.10$  nm; B)  $0.85 \pm 0.07$  nm).

40 nm wide for 0.50/0.50 DPPC/DLPC. Circular domains also coexist with the stripes in the case of 0.25/0.75 DPPC/DLPC deposited at higher surface pressure (Figure 1 A). The stripe formation mechanism has already been reported.<sup>[7]</sup> The area fraction covered by the stripes and circular domains, the measured step-height differences, and the mechanical responses of the domains observed by AFM phase imaging are consistent with phase separation into condensed DPPC-rich stripes and circles and a liquidlike, DLPC-rich background matrix.<sup>[15]</sup>

Figure 2 A shows the 0.25/0.75 DPPC/DLPC monolayer after the adsorption of delipidated HSA. A periodic array of grooves is observed in place of the protruding stripes. This is a result of preferential HSA adsorption to the fluid background matrix. From the higher magnification image shown in Figure 2 B, it can be clearly seen that the adsorbed protein molecules avoid the surface of the solidlike DPPC stripes. HSA adsorption was limited to the LE phase of DLPC by the choice of protein concentration and adsorption time. The mean depth of the grooves ( $1.7 \pm 0.3$  nm) and the step-height difference of the 0.25/0.75 DPPC/DLPC stripe pattern (0.89 nm) give a protein-layer thickness of  $\sim 2.6$  nm. This is consistent with a monolayer of protein adsorbed on the DLPC matrix, given that HSA has the shape of an equilateral triangle with  $\sim 8$ -nm sides and  $\sim 3$ -nm height.<sup>[6,16]</sup>

HGG adsorbs primarily to the DLPC matrix of the 0.25/0.75 DPPC/DLPC monolayer (Figure 3 A). In this case, the depth of the grooves is  $3.3 \pm 0.6$  nm. HGG is a Y-shaped protein, 14 nm in width, 10 nm in height, and 4.5 nm in thickness.<sup>[17–19]</sup> The adsorbed protein-layer thickness ( $\sim 4.2$  nm) deduced from the groove depth therefore suggests that the HGG molecules lie as a flat monolayer on the DLPC matrix.<sup>[18,20]</sup> The selective adsorption of HGG and its ability to aggregate Au nanoparticles in solution was exploited to direct the surface adsorption of the nanoparticles (Figure 3 B).<sup>[21]</sup> After nanoparticle ( $11 \pm 3$  nm diameter) adsorption to the HGG-covered DLPC matrix, the grooves are visibly narrower. A comparison of the cross-section analyses of Figure 3 A and B reveals an increase in the average groove depth from  $3.3 \pm 0.6$  nm to  $12.8 \pm 1.5$  nm. By comparison, exposure of the DPPC/DLPC monolayer surface to the Au colloid solution resulted in unselective adsorption.<sup>[15]</sup>

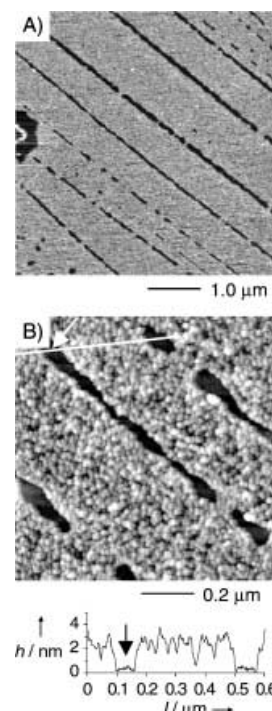


Figure 2. AFM images of HSA adsorbed on a DPPC/DLPC (0.25/0.75) monolayer (35 mN m<sup>-1</sup>): A) lower and B) higher magnification. Bottom: height-length profile for B). The arrow in B) indicates a “groove”. Grooves or depressions are not observed for mixed monolayers exposed to H<sub>2</sub>O.<sup>[15]</sup>

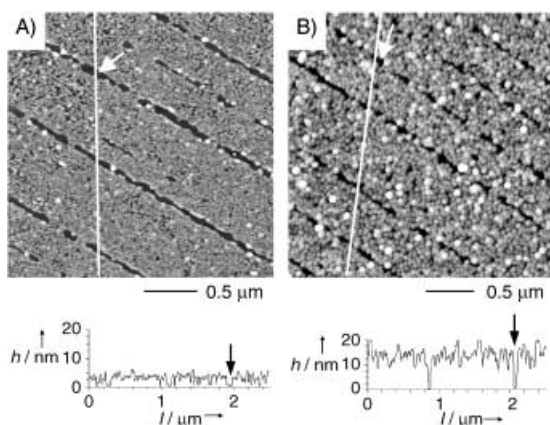


Figure 3. AFM images and height-length profiles of A) HGG adsorbed on a DPPC/DLPC (0.25/0.75) monolayer (35 mNm<sup>-1</sup>) and B) Au nanoparticles ( $d = 11$  nm) adsorbed on the HGG protein pattern (not the same area shown in A)).

The adsorption of HSA is sensitive to the phase state of the DPPC stripe domains, but that of HGG is not. This was established in the following way. HSA and HGG adsorption to a 0.50/0.50 DPPC/DLPC monolayer transferred at 15 mNm<sup>-1</sup> was investigated. Film transfer at this lower surface pressure produces DPPC stripes that are in the more disordered LC state.<sup>[12,14,22]</sup> Figure 4 shows the monolayer surface after HGG adsorption. HGG is primarily adsorbed to the DLPC matrix. The depth of the grooves is  $3.4 \pm 0.6$  nm, which gives an adsorbed HGG layer thickness of  $\sim 4.3$  nm. Au nanoparticles also adsorb selectively to the HGG-covered areas.<sup>[15]</sup> By contrast, HSA adsorbs to the surface of the DPPC stripes (Figure 5 A), thus resulting in a step-height difference of  $2.8 \pm 0.7$  nm. If HSA adsorbs to the DPPC stripes and the DLPC background to the same extent, a step-height difference of  $\sim 0.9$  nm would be expected. The AFM results instead suggest that HSA adsorbs to a greater extent to the LC phase of DPPC.

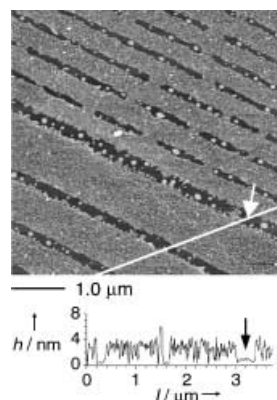


Figure 4. AFM image and height-length profile of HGG adsorbed on a DPPC/DLPC (0.50/0.50) monolayer transferred at 15 mNm<sup>-1</sup>. The spherical structures present on the DPPC stripes are probably desorbed phospholipid, as these are also observed for the mixed monolayer exposed to H<sub>2</sub>O.

For comparison, HSA adsorption to a 0.50/0.50 DPPC/DLPC monolayer deposited at 32 mNm<sup>-1</sup> was also investigated. In this case, the DPPC domains are in the SC phase. Grooves ( $2.2 \pm 0.3$  nm deep) are observed on the monolayer surface after exposure to HSA (Figure 5 B). A preferential adsorption of HSA to the LE matrix of DLPC is thus evident.

Overall, these results indicate that the surface adsorption of HSA is determined by the phase state of the template. This behavior can be explained by HSA interacting with the mixed monolayer surface through its alkyl-chain binding pockets.

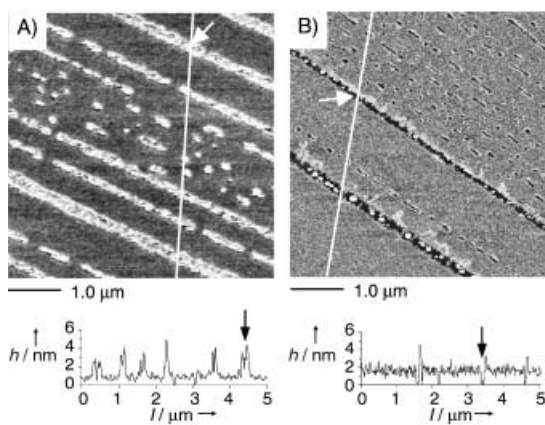


Figure 5. AFM images and height-length profiles of HSA adsorbed on a DPPC/DLPC (0.50/0.50) monolayer deposited at: A) 15 mNm<sup>-1</sup> and B) 32 mNm<sup>-1</sup>. The arrows indicate a protrusion in A) and a groove in B).

Previous studies report that the affinity and kinetics of HSA adsorption to alkylsilane monolayers are affected by the alkyl-chain packing density; HSA binds more strongly to loosely packed films.<sup>[9]</sup> This is consistent with the fact that the alkyl-chain packing density of DPPC ( $\sim 23.2\text{--}23.5$  Å<sup>2</sup>chain<sup>-1</sup>) in the SC stripes formed at 32–35 mNm<sup>-1</sup> prevents HSA from binding to the alkyl chains. HSA does bind to the more disordered LC phase of DPPC (15 mNm<sup>-1</sup>) because the lower alkyl-chain density ( $\sim 25$  Å<sup>2</sup>chain<sup>-1</sup>) allows HSA to interact directly with the alkyl chains, and not just with a surface of CH<sub>3</sub> groups.<sup>[9]</sup> The preferential adsorption of HSA to the LE matrix of DLPC in monolayers transferred at 32 or 35 mNm<sup>-1</sup> ( $\sim 29$  Å<sup>2</sup>chain<sup>-1</sup>) is consistent with this direct chain interaction.<sup>[20]</sup> HSA does not, however, effectively attach itself to the LE phase of DLPC (i.e. submonolayer coverage) when the alkyl chains are too loosely packed ( $\sim 35$  Å<sup>2</sup>chain<sup>-1</sup> in the 0.50/0.50 DPPC/DLPC film deposited at 15 mNm<sup>-1</sup>).

On the other hand, HGG adsorbs primarily to the LE phase of DLPC in the range of surface pressures and mixed monolayer compositions investigated in this study. A likely source of this selectivity is the inherent contrast in surface energies between the disordered LE phase of DLPC ( $\sim 31$  mJm<sup>-2</sup>) and the ordered LC or SC phases of DPPC ( $\sim 23$  mJm<sup>-2</sup>).<sup>[13]</sup> The preferential adsorption of HGG to the LE matrix of DLPC can be rationalized in terms of binding to the highest-energy sites available.<sup>[5,6,19]</sup>

In conclusion, we have used the selective adsorption of HSA and HGG to the LC or LE phase of a nanostructured LB monolayer of DPPC and DLPC to generate well-defined protein and Au nanoparticle/protein patterns. Whereas the usual approach to producing patterns and arrays of biomolecules involves chemically differentiated templates, we have shown in a proof-of-concept that patterning can be effected by using the solid/fluid-phase properties of coexisting domains on an organic film surface.

### Experimental Section

L-α-DPPC and L-α-DLPC were obtained from Avanti Polar Lipids (> 99%). Mixed DPPC/DLPC monolayers were deposited onto freshly cleaved mica by the LB technique, as previously described.<sup>[7]</sup>

Delipidated HSA (~99%) and HGG (99%) were obtained from Sigma. Aqueous HSA and HGG solutions (0.1 mg mL<sup>-1</sup>) were adsorbed to the DPPC/DLPC films at 23 °C by placing a sufficiently large drop of the protein solution to cover a surface of approximately 1 cm<sup>2</sup>. After 15 min, the drop was blown off of the surface by using N<sub>2(g)</sub>.

Au nanoparticles were prepared by the citrate reduction of HAuCl<sub>4</sub> (Aldrich).<sup>[23]</sup> A drop of the 10 nm Au-colloid solution was deposited on the protein-covered monolayer surface. After 5 min, the drop was blown off of the substrate surface. The surface was rinsed with a drop of H<sub>2</sub>O and blown dry.

AFM images were acquired in air (relative humidity = 25–30%, *T* = 21–24 °C) by using the tapping mode of a Nanoscope IIIa-MultiMode AFM (Digital Instruments) and etched Si cantilevers (resonance frequency = ~300 kHz, spring constant ~42 N m<sup>-1</sup>). A cantilever-oscillation amplitude of 60–65 mV and an oscillation damping of 15–25% were used.

Received: June 4, 2002 [Z19447]

- [1] M. Goren, R. B. Lennox, *Nano Lett.* **2001**, *1*, 735.
- [2] W. A. Hayes, C. Shannon, *Langmuir* **1998**, *14*, 1099.
- [3] T. Lee, N. Yao, I. A. Aksay, *Langmuir* **1997**, *13*, 3866.
- [4] R. W. Zehner, W. A. Lopes, T. L. Morkved, H. Jaegar, L. R. Sita, *Langmuir* **1998**, *14*, 241.
- [5] J. Frommer, R. Lüthli, E. Meyer, D. Anselmetti, M. Dreler, R. Overney, H.-J. Güntherodt, M. Fujihira, *Nature* **1993**, *364*, 198.
- [6] J. Fang, C. M. Knobler, *Langmuir* **1996**, *12*, 1368.
- [7] P. Moraille, A. Badia, *Langmuir* **2002**, *18*, 4414.
- [8] R. H. McMenamy, in *Albumin Structure, Function and Uses* (Eds.: V. M. Rosenoer, O. Murray, M. A. Rothschild), Pergamon, New York, **1977**.
- [9] a) S. Petrash, N. B. Sheller, W. Dando, M. D. Foster, *Langmuir* **1997**, *13*, 1881; b) S. Petrash, T. Cregger, B. Zhao, E. Pokidysheva, M. D. Foster, W. J. Brittain, V. Sevastianov, C. F. Majkrzak, *Langmuir* **2001**, *17*, 7645.
- [10] V. Silin, H. Weetall, D. J. Vanderah, *J. Colloid Interface Sci.* **1997**, *185*, 94.
- [11] S. Kidoaki, T. Matsuda, *Langmuir* **1999**, *15*, 7639.
- [12] K. S. Birdi, *Lipid and Biopolymer Monolayers at Liquid Interfaces*, Plenum, New York, **1989**.
- [13] C. E. H. Berger, K. O. van der Werf, R. P. H. Kooyman, B. G. de Grooth, J. Greve, *Langmuir* **1995**, *11*, 4188.
- [14] J. Hwang, L. K. Tamm, C. Böhm, T. S. Ramalingam, E. Betzig, M. Edidin, *Science* **1995**, *270*, 610.
- [15] See Supporting Information.
- [16] M. X. He, D. C. Carter, *Nature* **1992**, *358*, 209.
- [17] E. D. Day, *Advanced Immunochemistry*, 2nd ed., Wiley-Liss, New York, **1990**.
- [18] E. S. Grabbe, *Langmuir* **1993**, *9*, 1574.
- [19] A. Baszkin, D. J. Lyman, *J. Biomed. Mater. Res.* **1980**, *14*, 393.
- [20] As a result of AFM tip effects and changes in the protein conformation that occur upon adsorption and air drying, other HGG orientations are possible. For these same reasons, it was impossible to estimate the depth of HSA penetration into the lipid domains.
- [21] HGG can bind to Au through the asparagine subunits of its antigen-binding fragments or through the many S–S bonds that link its polypeptide chains.<sup>[17]</sup>
- [22] The 0.25/0.75 DPPC/DLPC monolayer is not phase-separated at 15 mN m<sup>-1</sup>.
- [23] K. C. Grabar, R. G. Freeman, M. B. Hommer, M. J. Natan, *Anal. Chem.* **1995**, *67*, 735.

## Topochemical Polymerization of 7,7,8,8-Tetrakis(methoxycarbonyl)quinodimethane

Takahito Itoh,\* Shinji Nomura, Takahiro Uno, Masataka Kubo, Kazuki Sada, and Mikiji Miyata\*

Topochemical polymerization, where the symmetry of the crystal lattice of the monomer is retained after polymerization, leads to a polymer with a highly controlled chemical structure because of the structural restraint imposed by the crystal lattice. This method is promising from the viewpoint of polymer structure control. However, monomers that can be polymerized topochemically are still limited because of the difficulties involved in controlling and predicting their crystal structures. Hasegawa reported topochemical polymerization reactions of 2,5-distyrylpyridine derivatives and related compounds and named them “four-centered photopolymerizations”.<sup>[1]</sup> Topochemical polymerizations of diacetylene derivatives were first reported by Wegner<sup>[2]</sup> and afterwards a large number of diacetylene derivatives<sup>[3]</sup> and triacetylene derivatives<sup>[4]</sup> were prepared and their corresponding polymers were investigated and found to have interesting optical and electronic properties.<sup>[5]</sup> More recently, Matsumoto et al. found that polymerization reactions of derivatives of muconic acid and derivatives of sorbic acid proceed topochemically.<sup>[6]</sup> They determined several parameters for the molecular stacking of the diene moieties, and explained the relationship between the topochemical polymerization and monomer packing in crystals for diene monomers.<sup>[6]</sup> Herein we report that the conjugated monomer 7,7,8,8-tetrakis(methoxycarbonyl)quinodimethane (**1**) can be polymerized topochemically.

The monomer **1** was originally synthesized by Acker and Hertler.<sup>[7]</sup> They briefly described its properties and noted that it oligomerized on heating or on leaving it to stand at room temperature in diffuse light to give pink materials which were insoluble in common organic solvents. Later, Iwatsuki and Itoh,<sup>[8]</sup> and Hall and Bentley<sup>[9]</sup> independently reported the polymerization behavior of **1** in solution. However, the polymer products of **1** were not given much attention and not well characterized because of their insolubility. These factors gave us an indication that **1** may undergo topochemical polymerization (Scheme 1).

The monomer **1** was prepared by a new synthetic route. Knoevenagel condensation of 1,4-cyclohexanedione with methyl malonate using titanium tetrachloride and pyridine as a dehydrating system afforded 1,4-[bis(methoxycarbonyl)-

[\*] Prof. Dr. T. Itoh, S. Nomura, Dr. T. Uno, Dr. M. Kubo  
Department of Chemistry for Materials  
Faculty of Engineering  
Mie University  
1515 Kamihama-cho, Tsu-shi, Mie 514-8507 (Japan)  
Fax: (+81) 59-231-9410  
E-mail: itoh@chem.mie-u.ac.jp  
  
Prof. Dr. M. Miyata, Dr. K. Sada  
Department of Material and Life Science  
Graduate School of Engineering  
Osaka University and Handai FRC  
2-1 Yamadaoka, Suita, Osaka 565-0871 (Japan)  
Fax: (+81) 6-6879-7406  
E-mail: miyata@mls.eng.osaka-u.ac.jp